Scientific paper

Influence of Alkali Cations (Me = Li, Na, K, Rb, Cs) on Physico-chemical Properties of the Liquid and Solid Phases of Me-aluminosilicate Hydrogels

Josip Bronić,[a]* Tatjana Antonić Jelić,[a] Ivan Krznarić,[a] Jasmina Kontrec,[a] Boris Subotić[a] and Gregor Mali[b]

[a]*Ruđer Bošković Institute, Bijenička 54, P.O.Box 180, 10002 Zagreb, Croatia*

[b]*National Institute of Chemistry, Hajdrihova 19, 1001 Ljubljana, Slovenia*

** Corresponding author: E-mail: josip.bronic@irb.hr*
Tel.: +385 145 60 991, Fax: +385 146 80 098

Received: 16-04-2008

Dedicated to the memory of Professor Ljubo Golič

Abstract

Me-alumosilicate hydrogels having the batch molar oxide composition $xMe_2O \times Al_2O_3 \times ySiO_2 \times zH_2O$ (Me = Li, Na, K, Rb and Cs); x = 4.24–4.66, y = 2.49 and z = 334.53–344.48 of the hydrogels (series a), and x = 9.52–10.30, y = 7.91–7.95 and z = 1073.38–1097.29 of the hydrogels (series b), were prepared by mixing of the appropriate Me-silicate and Me-aluminate solutions at room temperature. After ageing for 48 h at 25 °C and solid-liquid separation, the chemical compositions (contents of Me_2O, Al_2O_3 and SiO_2) of the liquid and solid phases were determined by AAS. Solid samples were additionally analyzed by XRD, FTIR and DTG. Specific equilibrium distributions of Me_2O, Al_2O_3 and SiO_2 between the solid and liquid phases were discussed in the terms of: (a) influence of Me ions on distribution of different silicate species and their degrees of hydroxylation in the starting Me-silicate solutions and (b) influence of the degrees of hydroxylation of silicate species in the starting Me-silicate solutions on the polycondensation reactions with monomeric $[Al(OH)_4]^-$ anions during the formation of the gel. The presence/absence of the formation of zeolite-like structures ("quasi-crystalline") in the gel matrix was discussed in the terms of the "structure-forming" nature of Li^+ and Na^+ ions and the "structure-breaking" character of K^+, Rb^+ and Cs^+ cations.

Keywords: Zeolite A, nucleation, hydrogels, "structure-breaking" cations, ageing

1. Introduction

A typical zeolite synthesis involves preparation and mixing together silicate and aluminate solutions (sols) to form the aluminosilicate hydrogel. Next step is transformation (hydrothermal treatment)[1–3] of the gel into zeolite(s). Particles of precipitated amorphous aluminosilicate (gel) are dispersed in the liquid phase of the hydrogel. Physico-chemical properties of hydrogels depend on the overall batch composition: $xMe_2O \times Al_2O_3 \times ySiO_2 \times zH_2O$ (Me = alkali cation) as well as on the way of gel preparation (order of addition of silicate and aluminate solutions, mode and intensity of stirring of the reaction mixture, time and temperature of precipitation, etc.)[1–11]. Changes in the conditions of the gel preparation, the use of different silica[11–13] sources, ageing[14] of the obtained hydrogel at room temperature, addition of alkaline[6,12,15–17] cations, and other above mentioned precipitation conditions can lead to different results with respect to the kinetics of crystallization, to the phase composition and to the particulate properties (particle size, particle size distribution, particle shape) of the crystalline end product.

It is well known that cations play a fundamental role in zeolite[18–22] crystallization. A unique structural characteristics of zeolite frameworks containing polyhedral cages, have led to the postulate that the cation stabilizes the formation of structural subunits that are precursors of the nucleating species[18] in zeolite crystallization. Because of their "structure-forming" or "structure-breaking" capacity toward water, cations can favor or inhibit the for-

mation of specific zeolitic structures by influencing the nature and configuration of various siliceous and aluminosilicate precursor[23] species. McCormic[24,25] *et al.* found that alkali metal cations influence the structure of dissolved silicate oligomers and silica condensation rate. Harvey and Dent Glasser[6] have observed that the concentration and type of alkali metal cation affect the formation of aluminosilicate gels – the precursor of zeolite formation. Il'in *et al.*[26] found that the type of alkali cation (Li^+, Na^+, K^+) considerably influences the composition and structural properties of hydrated precipitates in the processes of gelation, ageing, and hydrothermal treatment of silicates and aluminosilicates as well as on the crystallization of microporous silicates and aluminosilicates.

Hence, besides acting as counterions to balance the aluminosilicate framework charge, the inorganic cations present in a reaction mixture often appear as the dominant factors determining which structure[3,27,28] will be obtained, and at the same time may influence the pathway[12,15,21,29] of the crystallization process, crystal size[20,23,29–31] and morphology[23,30–35] of crystallized zeolite(s). These effects may be caused by: (a) formation of nuclei in the gel matrix[2,9,16,17,36–41] by structure-forming (Li^+, Na^+) and/or structure-breaking (K^+, Rb^+, Cs^+) actions of alkali[16,19–23,30–33,40] cations and (b) the influence of alkali cations on the formation of different silicate, aluminate and aluminosilicate species[6,23–26,42] in both the solid (gel) and the liquid phase of hydrogel, and thus on the critical processes of the zeolite crystallization (gel dissolution, nucleation and crystal growth).

Taking into consideration above mentioned, manifold influences of alkali cations on the aluminosilicate systems, the objective of this work is to investigate the influence of alkali cations on the distribution of Me_2O (Me = Li, Na, K, Rb and Cs), Al_2O_3 and SiO_2 between the solid and the liquid phase of Me-aluminosilicate hydrogels as well as on the chemical and (micro)structural properties of the solid phase of the hydrogels.

2. Experimental

2. 1. Preparation of Me-aluminate Solution

Aluminium wire (99.999% Al; Sigma-Aldrich) was used for preparation of aluminate solutions by dissolving it in appropriate LiOH (analytical grade, Kemika), NaOH (analytical grade, Kemika), KOH (analytical grade, Kemika), RbOH (50 wt. % water solution; Sigma-Aldrich) and CsOH (purrum, ≥95 wt. % CsOH × H_2O, Fluka) solutions. Aluminum wire was completely dissolved in LiOH, NaOH, KOH, RbOH and CsOH, under reflux at 100 °C, so that the corresponding Li-, Na-, K-, Rb- and Cs-aluminate solutions were clear and transparent. However, a part of aluminium dissolved in LiOH was precipitated in the form of $Al(OH)_3$ during the cooling of the solution A1a to the ambient temperature. The resulting mole oxide compositions of the corresponding Me-aluminate suspension/solutions are shown in Table 1.

Table 1. Chemical composition of the starting aluminate solutions.

System	Me	Me_2O	Al_2O_3	H_2O
A1a	Li	1.90	1.00	172.55
A1b	Li	1.90	1.00	550.63
A2a	Na	2.01	1.00	172.55
A2b	Na	2.00	1.00	551.09
A3a	K	2.07	1.00	172.55
A3b	K	2.06	1.00	550.54
A4a	Rb	2.01	1.00	172.55
A4b	Rb	2.02	1.00	550.63
A5a	Cs	2.01	1.00	175.55
A5b	Cs	2.00	1.00	548.62

2. 2. Preparation of Me-silicate Solution

Fumed silica (99.8% SiO_2, Sigma-Aldrich) was used for preparation the silicate solutions by dissolving it in appropriate LiOH, NaOH, KOH, RbOH and CsOH solutions. It was completely dissolved and the corresponding Me-silicate solutions were clear and transparent. The resulting oxide compositions of the corresponding solutions are shown in Table 2.

Table 2. Chemical composition of the starting silicate solutions.

System	Me	Me_2O	SiO_2	H_2O
S1	Li	0.94	1.00	69.39
S2	Na	1.01	1.00	69.30
S3	K	1.04	1.00	69.33
S4	Rb	1.04	1.00	69.39
S5	Cs	1.04	1.00	69.39

2. 3. Preparation of Me-aluminosilicate Hydrogels

All aluminate (except the suspension A1a) and silicate solutions were filtered through 0.8 μm filtration membranes and thermostated at 25 °C prior to mixing. Alumosilicate hydrogels were prepared by pipetting of certain amount of the Me-silicate solution into a plastic

Table 3. Chemical composition of the starting hydrogels.

System	Me	Me_2O	Al_2O_3	SiO_2	H_2O
HG1a	Li	4.24	1.00	2.49	344.48
HG1b	Li	9.52	1.00	7.94	1090.08
HG2a	Na	4.51	1.00	2.49	343.69
HG2b	Na	10.02	1.00	7.95	1097.29
HG3a	K	4.66	1.00	2.49	334.53
HG3b	K	10.30	1.00	7.94	1078.45
HG4a	Rb	4.52	1.00	2.49	340.14
HG4b	Rb	10.04	1.00	7.94	1090.70
HG5a	Cs	4.52	1.00	2.49	344.31
HG5b	Cs	9.99	1.00	7.91	1073.38

beaker containing 50 ml of the appropriate Me-aluminate solution stirred by a propeller. The batch molar oxide compositions are shown in Table 3.

2. 4. Treatment of the Hydrogels

The hydrogels aged in cuvettes (48 h at 25 °C) were centrifuged to separate the solid from the liquid phase. A part of the clear liquid phase (supernatant) was used for measuring the concentrations of cations, aluminum and silicon by atomic absorption spectroscopy. The rest of the supernatant was carefully removed without the disturbance of the solid phase (sediment). After removal of the supernatant, the solid phase was redispersed in doubly distilled water and centrifuged repeatedly. The procedure was repeated until the pH value of the liquid phase above the sediment was 9. Cuvettes with the wet, washed solids were dried overnight at 105 °C and cooled in a desiccator over silicagel and weighted. Thereafter, the solids were removed from the cuvettes and were pulverized in agate mortar. The pulverized solid samples were kept in a desiccator with saturated NaCl solution for 96 h. Such prepared solids were used for: chemical analysis, X-ray diffraction (XRD), Fourier-transform infrared spectroscopy (FTIR), thermogravimetry (TG) and differential thermogravimetry (DTG). A part of each sample was calcined at 800 °C for 2 h. After cooling to ambient temperature (in a desiccator over dry silicagel), a given amount of each of the calcined samples was dissolved in 1:1 HCl solution. The obtained solutions were diluted with distilled water to the concentration ranges suitable for measuring the concentrations of Li, Na, K, Rb, Cs, Al and Si by atomic absorption spectroscopy (AAS).

2. 5. Analysis of Samples

^{29}Si-NMR (recorded at 300 MHz Varian Inova spectrometer, equipped with a Varian liquids probe) was used to characterize the silicate anions distribution in silicate solutions S1, S2, S3, S4 and S5. The X-ray diffractograms of all solid samples were made by Philips PW 1820 (CuK_α radiation, 2 Θ = 5–50 degrees). IR transmission spectra of the samples were made by the KBr wafer technique on the System 2000 (Perkin-Elmer) FTIR spectrometer. TG and DTG analysis, of the gels was made by TA 4000 System (Mettler-Toledo) apparatus. Concentrations of alkali cations, Al and Si in the solutions were measured by the Perkin-Elmer 3030B AAS.

3. Results and Discussion

Fig. 1 shows the ^{29}Si-NMR spectra of Me-silicate solutions S1–S5 which are, at first sight, similar. But more detailed analysis of the spectra shows differences in the distribution of different silicate species among the analyzed Me-silicate solutions. Table 4 shows that percentage of monomers is about the same (above 41%) in Li-silicate

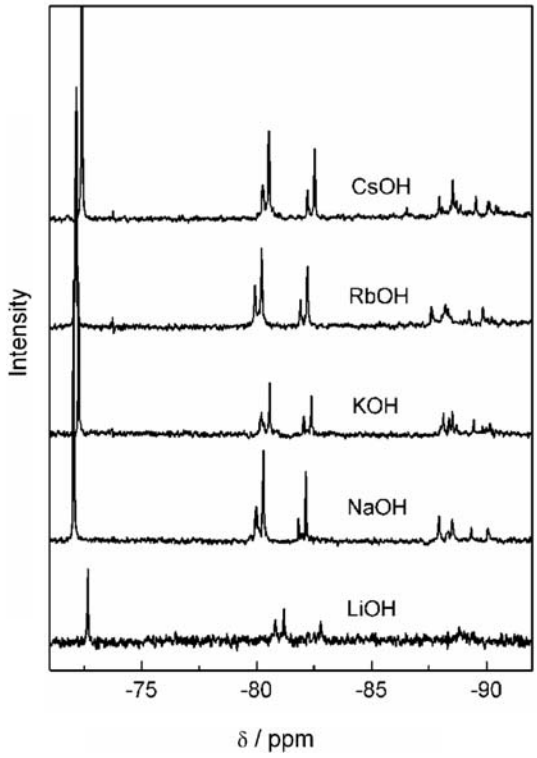

Fig. 1. ^{29}Si-NMR spectra of Me-silicate solutions prepared using appropriate hydroxides: S1 (LiOH), S2 (NaOH), S3 (KOH), S4 (RbOH), and S5 (CsOH).

Table 4. Distribution of different silicate species in the Me-silicate solutions S1 – S5.

Solution	**S1** **Li**	**S2** **Na**	**S3** **K**	**S4** **Rb**	**S5** **Cs**
monomer	43.5	41.2	36.2	32.0	31.7
dimer	35.6	15.0	15.7	12.8	15.6
linear trimer + linear tetramer + branched cyclic trimer	–	16.4	9.5	11.6	10.3
cyclic trimer	12.0	9.3	9.6	8.8	9.3
cyclic tetramer	–	11.3	11.0	12.6	14.0
branched cyclic tetramer	8.9	–	5.7	8.1	6.6
bicyclic pentamer	–	4.6	5.4	5.7	4.4
prismatic hexamer	–	2.2	6.6	8.7	8.1

and Na-silicate solutions, and is considerably lower (31.7–36.2%) in K-, Rb- and Cs-aluminate solutions. On the other hand, percentages of dimers in Na-, K-, Rb- and Cs-silicate solutions are similar (13–16%), and considerably lower than in Li-aluminate solution (35.6%). Except Li-silicate solution (S1), the percentages of other silicate species do not differ considerably among different Me-silicate solutions (see Table 4).

An analysis of connectivity distribution[43] (see Table 5) shows that lower degrees of connectivity (Q^o, Q^1) changes in the sequence: $(Q^n)_{Li} > (Q^n)_{Na} > (Q^n)_K \approx (Q^n)_{Cs} \approx (Q^n)_{Rb}$. Due to relatively low percentages of linear trimer and linear tetramer in all solutions (9.5–16% in the mixture: linear trimer + linear tetramer + branched cyclic trimer; see Table 4), the degree of connectivity Q^2 is relatively low in these solutions (see Table 5); even, absence

Table 5. Connectivity distribution of silicate species in the Me-silicate solutions S1–S5.

	Connectivity (%)				
Cation	Q^o	Q^1	Q^2	Q^2_Δ	Q^3_Δ
Li^+	21.9	41.3	–	32.3	4.5
Na^+	17.1	23.9	6.9	40.6	11.5
K^+	13.3	19.5	3.5	41.6	22.1
Rb^+	10.8	17.9	3.9	42.0	25.4
Cs^+	11.0	19.1	3.6	42.9	23.6

of linear trimer and linear tetramer in the Li-silicate solution causes the absence of connectivity Q^2 in this solution. On the other hand, higher degrees of connectivity (Q^2_Δ and Q^3_Δ), caused by the presence of cyclic silicate species (cyclic trimer, branched cyclic trimer, cyclic tetramer, branched cyclic tetramer, bicyclic pentamer and prismatic hexamer; see Table 4) changes in the sequence: $(Q^n_\Delta)_{Li} < (Q^n_\Delta)_{Na} \approx (Q^n_\Delta)_K \approx (Q^n_\Delta)_{Cs} \approx (Q^n_\Delta)_{Rb}$ for n = 2 and in the sequence: $(Q^n_\Delta)_{Li} < (Q^n_\Delta)_{Na} < (Q^n_\Delta)_K \approx (Q^n_\Delta)_{Cs} \approx (Q^n_\Delta)_{Rb}$ for n = 3. The low content of the connectivity Q^3_Δ in the Li-silicate solution (4.5%) relative to the content of the connectivity Q^3_Δ in Na-silicate solution (11.5%), and especially in the K-, Cs- and Rb-silicate solutions (22–25%) is caused by the absence of bicyclic pentamer and prismatic hexamer in the Li-silicate solution (see Table 4).

Based on the analysis of the connectivity distribution in different Me-silicate solutions, Bell[43] postulated that extent of oligomerization of silicate species in solution increases with increasing cation size, and that this effect is caused by the formation of cation-anion pairs which stabilize the anionic species[24,25] to the hydrolysis. However, analysis of the distribution of silicate species (Table 4) and connectivity of the silicate species (Table 5) in the silicate solutions S1–S5 shows that extent of oligomerization (EO_{Me}) decreases only in the sequence: $EO_{Li} < EO_{Na} < EO_K$, but that the extent of oligomerization is almost the same in the K-, Cs- and Rb-silicate solutions, i.e. $EO_K \approx EO_{Rb} \approx EO_{Cs}$. This difference is probably caused by the distinction in total concentration of SiO_2 and $R = [SiO_2]/[Me_2O]$. The total concentration of SiO_2 is 3 mol % and $R = 2$ in the silicate solutions studied by Bell[43], while the total concentration of SiO_2 is 1.4 mol % and $R = 1$ in the Me-silicate solutions S1–S5. Hence, it seems that change (increase) of the extent of oligomerization with increased cation size becomes less expressive as concentration of SiO_2 decreases and concentration of Me_2O simultaneously increases.

Here, it is interesting that at least two groups of cations can be recognized on the basis of analysis of distribution of silicate species (Table 4) and their connectivity (Table 5); structure-forming cations (Li^+ and Na^+) and structure-breaking cations (K^+, Cs^+ and Rb^+)[16,17,20,26,30,40]. Even, among the same "structure-forming" group, Li^+ ion exhibit a specific behavior indicated by a high content of monomers and dimers, and absence of linear trimer, linear tetramer, branched cyclic trimer, cyclic tetramer, bicyclic pentamer and prismatic hexamer (see Table 4). This is probably caused by formation of ionic pairs[24,25,43] between highly negative charged silicate monomers and dimers and small, strongly polarizing Li^+ ions,[44–47] and thus their stabilization.

The X-ray diffraction patterns of the solids G1a–G5a, separated from the hydrogels HG2a–HG5a (Fig. 2A)

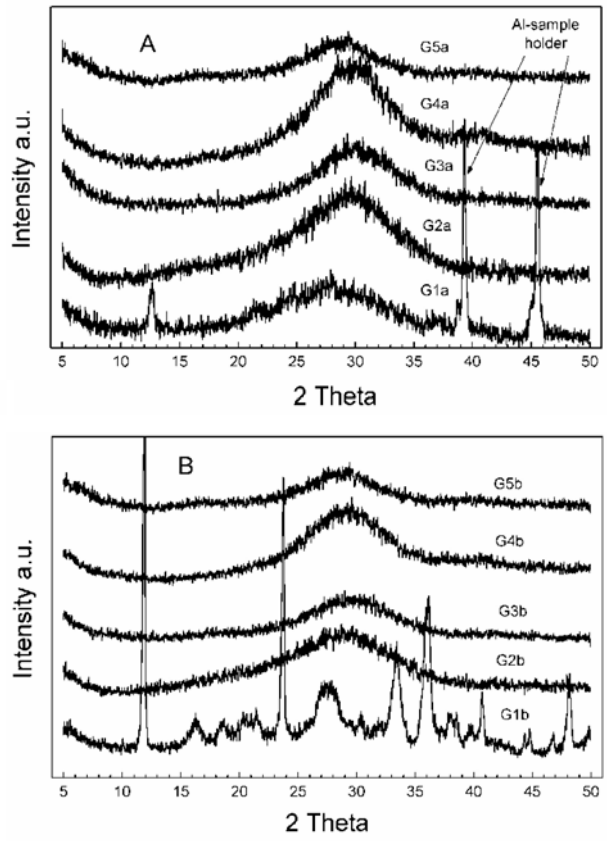

Fig. 2. X-ray diffraction patterns of gels from system a (A) and from system b (B), prepared from corresponding MeOH: G1 (LiOH), G2 (NaOH), G3 (KOH), G4 (RbOH), G5 (CsOH).

and G1b–G5b, separated from the hydrogels HG1b–HG5b (Fig 2B) are specified by a broad "maxima" at about $2\theta = 30°$, characteristic for true amorphous[48–51] precipitated aluminosilicates. Amorphous nature of the samples is also revealed by FTIR analysis. IR spectra show intense bands of zeolite skeleton structural units of even a few unit cels[52]. The absence of the intense band characteristic for crystalline phase(s) (zeolite(s))[53] in the FTIR spectra of the solids G2a–G5a (Fig. 3A) and G1b–G5B (Fig. 3B) reveals that the specific profile of the X-ray spectra in Fig. 2 are caused by true amorphous nature of the corresponding samples, and not by low amount of the crystalline phase and/or lowering of crystal size below X-ray detection limit[40,54].

Similarity of the X-ray diffraction patterns (Fig. 2) as well as FTIR spectra (Fig. 3) of the samples G2a–G5a and G2b–G5b indicates that the aluminosilicate framework "structure" which determines their amorphous character (at least for those sensitive to XRD and FTIR) is not considerably influenced either by the type of alkali cation or by the SiO_2/Al_2O_3 ratio of the solid phase (see Table 3). Specificities of the samples G1a (Me = Li) expressed by the difference of its X-ray diffraction pattern (Fig. 2) and FTIR spectrum (Fig. 3) relative to the X-ray diffraction patterns and FTIR spectra of other solids (G2a–G5a and G1b–G5b) are probably caused by precipitation of $Al(OH)_3$ during heating-cooling of the "solution" A1a (dissolution of LiOH, see Experimental).

The quantity of the precipitated solid phase (gel) within hydrogel as well as their oxide composition and molar ratio to Al_2O_3 are shown in Table 6. Distribution of aluminium between the solid and the liquid phase (excluding the suspension HG1a, which will be discussed separately) is in accordance with the previous finding[8]: In a batch system with given molar concentration of silicon dioxide ($[SiO_2]_b$), the amount of the Al_2O_3 contained in the solid phase ($[Al_2O_3]_S$), is directly proportional to the molar batch concentration ($[Al_2O_3]_b$) of aluminium oxide and inversely proportional to the molar batch concentration of alkali metal oxide ($[Me_2O]_b$), i.e.,

$$[Al_2O_3]_S = k_1 + k_2[Al_2O_3]_b/[Me_2O]_b \quad (1)$$

where k_1 and k_2 are constants which depend on $[SiO_2]_b$.

Mass fractions of oxides (Me_2O, Al_2O_3, SiO_2) of the solid phase (f_S) in comparison to the total oxides content

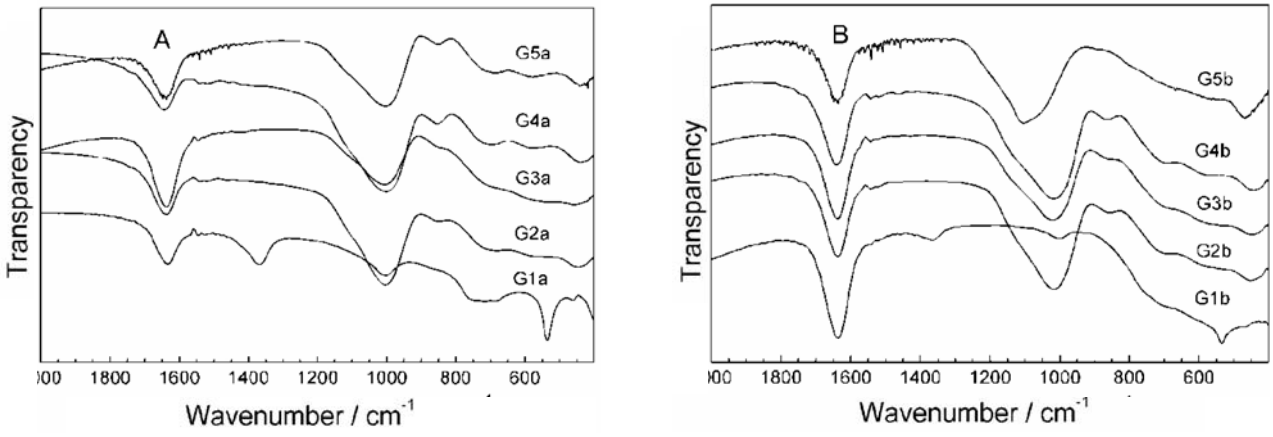

Fig. 3. FTIR spectra of gels from system a (A) and from system b (B), prepared from corresponding MeOH: G1 (LiOH), G2 (NaOH), G3 (KOH), G4 (RbOH), G5 (CsOH).

Table 6. Amounts of the (X-ray amorphous) solid phases (a_G) in wt. % relative to the amount of hydrogel, their chemical composition, wt. % of Me_2O, Al_2O_3, SiO_2, H_2O, and their molar ratios to the Al_2O_3: $x = Me_2O/Al_2O_3$, $y = SiO_2/Al_2O_3$ and $z = H_2O/Al_2O_3$).

Solid phase	a_G (wt. %)	Me_2O	Al_2O_3	SiO_2	H_2O	x	y	z
G1a (Li)	2.120	3.26	41.43	1.57	53.74	0.27	0.06	7.34
G1b (Li)	1.40	8.32	28.21	50.36	13.11	1.00	3.03	2.63
G2a (Na)	3.75	15.63	24.65	36.56	23.16	1.04	2.52	5.32
G2b (Na)	1.62	13.83	20.87	42.07	23.23	1.09	3.42	6.29
G3a (K)	4.11	19.14	22.84	37.89	20.13	0.91	2.82	4.99
G3b (K)	1.84	17.34	19.16	42.99	20.51	0.98	3.80	6.06
G4a (Rb)	4.56	32.05	16.80	30.50	20.65	1.04	3.08	6.96
G4b (Rb)	2.13	28.39	14.19	35.40	22.02	1.09	4.23	8.78
G5a (Cs)	5.70	43.02	13.49	26.29	17.20	1.15	3.31	7.22
G5b (Cs)	2.43	39.95	11.90	35.49	12.66	1.21	5.06	7.63

Table 7. Mass fractions of Me_2O, Al_2O_3 and SiO_2 of the solid phase (f_S(oxide)) in hydrogel and their distribution between solid and liquid phase R(oxide) = f_S(oxide)/f_L(oxide).

Hydrogel	$f_S(Me_2O)$	$f_S(Al_2O_3)$	$f_S(SiO_2)$	$R(Me_2O)$	$R(Al_2O_3)$	$R(SiO_2)$
HG1a (Li)	0.036	0.567	0.015	0.037	1.358	0.015
HG1b (Li)	0.072	0.681	0.260	0.078	2.134	0.035
HG2a (Na)	0.141	0.610	0.616	0.164	1.564	1.604
HG2b (Na)	0.076	0.696	0.299	0.082	2.289	0.427
HG3a (K)	0.120	0.618	0.698	0.136	1.617	2.310
HG3b (K)	0.069	0.725	0.348	0.074	2.630	0.533
HG4a (Rb)	0.124	0.543	0.672	0.141	1.188	2.049
HG4b (Rb)	0.071	0.656	0.350	0.076	1.907	0.538
HG5a (Cs)	0.148	0.583	0.775	0.173	1.398	3.444
HG5b (Cs)	0.076	0.645	0.413	0.082	1.817	0.704

within hydrogels and their distribution (R) between solid and liquid phase (f_L) are shown in Table 7. Here, f_S(oxide) = (amount of oxide in the solid phase)/(total amount of oxide in hydrogel), f_L(oxide) = (amount of oxide in the liquid phase)/(total amount of oxide in hydrogel), and R(oxide) = f_S(oxide)/f_L(oxide). Except in the suspension HG1a, distribution of alkali metal cations Me^+ between the solid and the liquid phase of hydrogel does not depend on the nature of cation and lies between 0.136 and 0.173 for the hydrogels of series a, and between 0.074 and 0.082 for the hydrogels of series b (Table 7).

Low fractions $f_S(Me_2O)$ (an average of 0.133 for the hydrogels of series a and 0.078 for the hydrogels of series b) and consequently low values of $R(Me_2O)$ are caused by the high batch ratios $[Me_2O/Al_2O_3]_b$ (about 4.5 for the hydrogels of series a and about 10 for the hydrogels of series b; see the composition of hydrogels in Table 3.) relative to the low ratio $[Me_2O]_S/[Al_2O_3]_S$ ($x \approx 1$; see Table 6) in the solid phase of hydrogel. For the same reason, $R(Me_2O)$ for the hydrogels of series a is about two times higher than the $R(Me_2O)$ for the hydrogels of series b (see Table 7).

Low value of $f_S(SiO_2)$ in the suspension HG1a (see Table 6) indicates that, due to the precipitation of "free" Al-oxides, most of SiO_2 is not bonded with Al_2O_3 through common oxygen atoms. Therefore, only a small fraction of Li ions is present in the solid phase as compensating cations, i.e. most of lithium ions are present in the liquid phase, as it is indicated by low values of $f_S(Li_2O)$ and $R(Li_2O)$ (see Table 7).

Introducing characteristic values (see Table 4 in Ref. 8) of batch oxide concentrations and constants, listed in Table 8., into Eq. (1), one can calculate that: $[Al_2O_3]_S = 0.1085$ mol dm^{-3} for the hydrogels of series a and $[Al_2O_3]_S = 0.038$ mol dm^{-3} for the hydrogels of series b, and thus $f_S(Al_2O_3) = 0.68$ for hydrogels of series a and $f_S(Al_2O_3) = 0.75$ for hydrogels of series b. These values are very close to the upper marginal values of $f_S(Al_2O_3)$ (0.62 and 0.73 for hydrogels of series a and b, respectively, see Table 7). It shows that the amount of Al_2O_3 in the solid phase is determined by the relationship between the

Table 8. Characteristic batch concentrations of $[Me_2O_b]$, $[Al_2O_{3b}]$, and $[SiO_2]_b$, and values of constants k_1 and k_2.

	Series a mol dm^{-3}	Series b mol dm^{-3}
$[Me_2O]_b$	0.7284	0.5095
$[Al_2O_3]_b$	0.1600	0.0505
$[SiO_2]_b$	0.4000	0.4000
k_1	–0.0200	–0.0200
k_2	0.5850	0.5850

batch molar concentrations $[Al_2O_3]_b$, $[Me_2O]_b$ and $[SiO_2]_b$ defined by Eq. (1).

The content of aluminosilicate ($a_G(Al_2O_3)$ + $a_G(SiO_2)$) in the precipitated solids, normalized to the percentage of mass of corresponding hydrogel (a_G–$a_G(Me_2O)$ –$a_G(H_2O)$) is ca. 2.3 wt.% for gels G2a–G5a and ca. 1.1 wt. % for gels G2b–G5b. Within series (except for G1a and G1b) amount of alumosilicate in hydrogels is constant and does not depend on the nature of cation. Since $(Me_2O)_S/(Al_2O_3)_S \approx 1$ = constant (except for G1a, see Table 7), the increase of the amount (a_G) of the precipitated solid in the sequence: $a_G(Li) < a_G(Na) < a_G(K) < a_G(Rb) < a_G(Cs)$, obviously arise as a consequence of an increase of the molecular mass of the Me_2O in the same sequence. On the other hand, the lower amounts of the solid phase of series b (a_G(b)) relative to the amounts of gel in series a (a_G(a)) were expected due to lower aluminosilicate concentrations in the hydrogels of series b than in series a [$a_G(a)/a_G(b) = 2.25 \pm 0.10$)]. The values, $(Me_2O)_S/(Al_2O_3)_S \approx 1$ (except for Me = Li in suspension HG1a; see Table 7) indicate that Al in the skeleton of amorphous aluminosilicate gel is coordinated four-fold within the common (Si, Al, O)-framework[2,55,56], whereas the Me^+ ions compensate the excess of negative charges of aluminum-oxygen tetrahedra[2]. Hence, the values $Me_2O/Al_2O_3 > 1$, obtained for the gels G2a, G2b, G4a, G4b, G5a and G5b (see Table 6) are probably the consequence of insufficient washing of solids, leaving a portion of MeOH in the gel micropores[7–11,16].

While the lower contents of Al_2O_3 and consequently, higher ratios $(SiO_2)_S/(Al_2O_3)_S$ in the gels of series b than

in the gels of series a, can be readily explained[1–3,7–11,57–60] by higher ratios $[SiO_2/Al_2O_3]_b$ in hydrogels (see Experimental), a continuous decrease in the Al_2O_3 content from Li-gels (G1a and G1b) to Cs-gels (G5a and G5b) is obviously affected by the nature of cation. Since the aluminate solutions contain only $[Al(OH)_4]^-$ ions at high pH[3,6,42,61,62], it is evident that the $(SiO_2)_S/(Al_2O_3)_S$ in the precipitate is determined by the distribution of different silicate species in the starting Me-silicate solutions (S1–S5; see Table 6), and thus by the type of alkali cation. Results of the ^{29}Si-NMR spectroscopy of the gels, prepared with different alkali metal cations, provide direct evidence for the presence of cation-silicate anion pairs, and indicate that the extent of pair formation increases with increasing cation size. The formation of such pairs stabilizes the anionic species to hydrolysis and explains the increase in oligomerization with increasing pair formation[43]. Hence, the increase of the molar ratio $(SiO_2)_S/(Al_2O_3)_S$ in the precipitate with the increasing cation size can be explained in terms of: (I) the polycondensation mechanism of formation of aluminosilicate gel skeleton[1] from monomeric $[Al(OH)_4]^-$ anions and silicate anions with different degrees of hydroxylation[3,25,29–32,63,64] and (II) an observation that, aluminum species were preferentially complexed with the larger species almost immediately, in solutions containing a mixture of silicate species. However, the subsequent polymerization of those complexes was slow[6].

Appearance of two endothermic minima in the DTG curves of the gels G1b (Fig. 4A), G2a and G2b (Fig. 4B) is in accordance with our previous DTG analyzes of aluminosilicate gels containing different proportions[16,40] of Li^+, Na^+ and K^+ ions. The first ("low-temperature") peak at 70–80 °C (see Fig. 4) corresponds to the removal of loosely held moisture from the solid microstructure[9,16,40]. On the other hand, the position of the second ("high-temperature") peak in DTG curves of the gels G2a, G1b and G2b (ca. 150 °C; see Fig. 4) was similar to the peak positions in DTG curves of zeolites (120–170 °C)[9,16,40]. Therefore, it is evident that the presence of "structure-forming" ions (Li^+, Na^+)[20,2630] in the batch system induces the formation of structural subunits or even more complex zeolite-like structures ("quasi-crystalline" phase) [65] inside the gel matrix, during its formation[16,40]. DTG curves of the potassium gels (G3a and G3b at Fig. 4) exibit an expressive "low temperature" peak and a very weak "shoulder" on the position of the high-temperature peaks, showing a slight ability of K^+ ions for the formation of "quasi-crystalline" phase in the gel matrix[16,40]. The absence of the "high-temperature" endothermic minima in DTG curves of the rubidium and cesium gels (G4a, G4b, G5a and G5b) was expected because of the "structure-breaking" nature of the compensation Rb^+ and Cs^+ cations[16,19–23,30–33].

4. Conclusions

Analysis of the ^{29}Si-NMR spectra of the Me-silicate solutions S1–S5, used for the preparation of hydrogels of series a (HG1a–HG5a) and series b (HG1b–Hg5b) have shown that percentage of monomers in silicate solutions

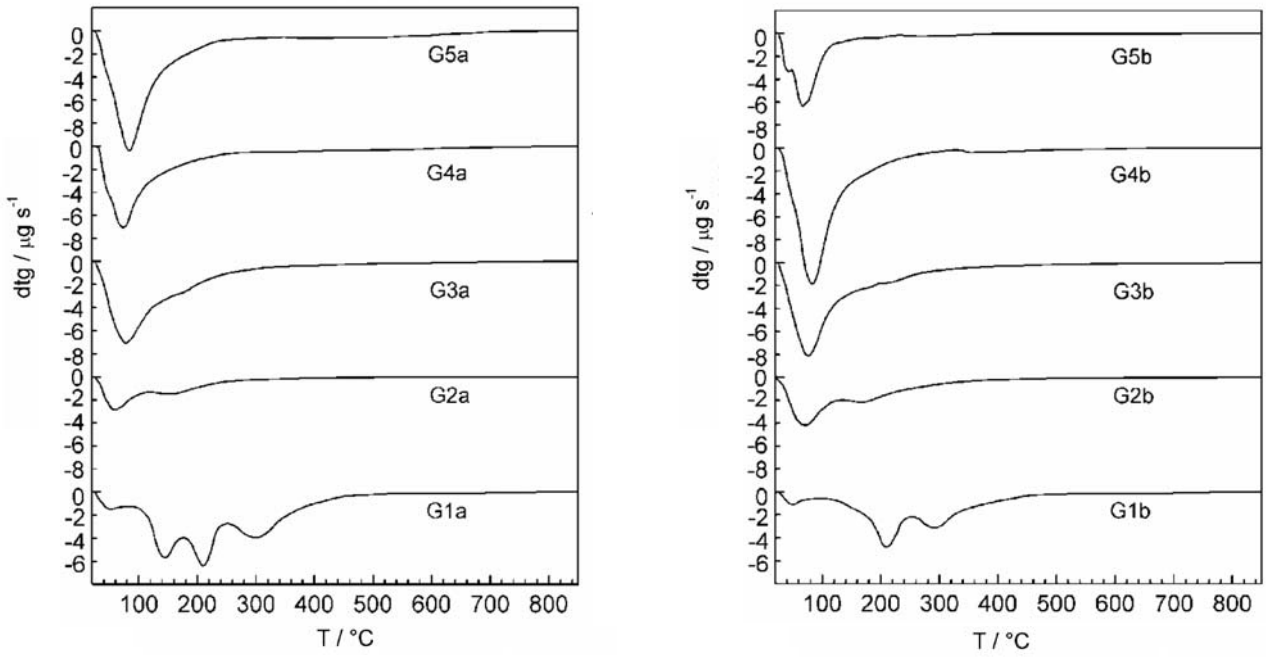

Fig. 4. DTG curves of the solid phases (gels) of system a (left) and of system b (right), prepared from corresponding MeOH: G1 (LiOH), G2 (NaOH), G3 (KOH), G4 (RbOH), G5 (CsOH).

decreases from 43.5% in S1 (LiOH) to 31.7% in S5 (CsOH), while the percentage of dimers (except in S1) is about the same in all solutions (S2–S5). Except in Li-silicate solution (S1), the percentages of other silicate species (linear trimer, linear tetramer, cyclic trimer, cyclic tetramer, bicyclic pentamer and prismatic hexamer) do not differ considerably among different Me-silicate solutions (Me = Li, Na, K, Rb and Cs). In literature is postulated that degree of connectivity distribution (Q^n), and thus the extent of oligomerization (EO_{Me}) of silicate species in solution, increases with increasing cation size. Our analyses have shown that extent of oligomerization decreases only in the sequence: $EO_{Li} < EO_{Na} < EO_{K}$. The extent of oligomerization is almost the same in the K-, Cs- and Rb-silicate solutions, i.e. $EO_{K} \approx EO_{Rb} \approx EO_{Cs}$. Hence, at least two groups of cations can be recognized on the basis of analysis of distribution of silicate species, and their connectivity (extent of oligomerization): "structure-forming cations" (Li^+ and Na^+) and "structure-breaking cations" (K^+, Cs^+ and Rb^+).

The solid phases of the hydrogels (HG1a–HG5a and HG2b–HG5b), formed by mixing together the silicate solutions S1–S5 with appropriate aluminate solutions, are truly amorphous Me-aluminosilicates as revealed by their X-ray diffractograms and FTIR spectra analysis.

The distribution of cations (Me) between the solid and the liquid phase of hydrogel does not depend on the nature of cation. The amount of Al_2O_3 contained in the solid phase (gel) makes the distribution of Me-cations, between the solid and liquid phase of hydrogel, directly proportional to the molar batch concentration of Al_2O_3 ($[Al_2O_3]_b$) and inversely proportional to the molar batch concentration of alkali metal oxide $[Me_2O]_b$. The amount of Al_2O_3 in the solid phase can be calculated using Eq. (1).

The increase of the molar ratio SiO_2/Al_2O_3 in the precipitate with the increasing cation size can be explained in terms of the polycondensation mechanism of formation of aluminosilicate gel skeleton from monomeric $[Al(OH)_4]^-$ anions and silicate anions with different degrees of hydroxylation and by the fact that aluminum species preferentially made complexes (react faster) with larger silicate species, in solutions containing a mixture of silicate species.

DTG analysis of the gels indicates that the presence of "structure-forming" ions (Li^+, Na^+) in the batch systems induces the formation of local order structure (sub)units ("quasi-crystalline" phase) within gel matrix, during its formation. Since the "quasi-crystalline" phase represents the potential nuclei that can start to grow after their releasing from the gel matrix (dissolved during its hydrothermal treatment) and being in the full contact with the liquid phase, this thesis will be evaluated in our further studies relating to hydrothermal treatment of hydrogels as well as the solids (gels) separated from the hydrogels.

5. Acknowledgement

This work was realized in the frame of the Project 0982904-2953 of the Croatian Ministry of Science, Education and Sports and Slovenian Ministry of Higher Education, Science and Technology.

6. References

1. D. W. Breck, *J. Chem. Educ.*, **1964,** *41*, 678–689.
2. S. P. Zhdanov in: R.F. Gould (Ed.), *Molecular Sieve Zeolites – I, Advances in Chemistry Series No. 101*, American Chemical Society, Washington, D.C., **1971,** p. 20
3. R. M. Barrer, *Hydrothermal Chemistry of Zeolites*, Academic Press, London, **1982,** p. 120.
4. G. T. Kerr, *J. Phys. Chem.*, **1968,** *72,* 1385–89.
5. F. Polak and A. Cichocki, In: *Molecular Sieves Zeolites – I.* (Eds.; L. B. Sand, E. M. Flanigen); Advances in Chemistry Series 121; American Chemical Society: Washington, DC, **1973;** *209.*
6. G. Harvey and L. S. Dent Glasser in: M. L. Occelli, H. E. Robson (Eds.), *Zeolite Synthesis, American Chemical Society Symposium Series no. 398*, American Chemical Society, Washington, D.C., **1989,** 49–65.
7. I. Krznarić, T. Antonić and B. Subotić, *Zeolites*, **1997,** *19,* 29–36.
8. I. Krznarić, T. Antonić and B. Subotić, *Microporous Mesoporous Mater.*, **1998,** *20,* 161–75.
9. I. Krznarić, T. Antonić, B. Subotić and V. Babić-Ivančić, *Thermochimica Acta*, **1998,** *317,* 73–84.
10. I. Krznarić, B. Subotić, *Microporous Mesoporous Mater.*, **1999,** *28,* 415–425.
11. I. Krznarić, T. Antonić, J. Bronić, B. Subotić and R.W. Thompson, *Croat. Chem. Acta*, **2003,** *76,* 7–17.
12. W. Meise and F. E. Swochow, In: *Molecular Sieves Zeolites – I.* (Eds.; L. B. Sand, E. M. Flanigen); Advances in Chemistry Series 121; American Chemical Society: Washington, DC, **1973;** 169.
13. K. E. Hamilton, E. N. Coker, A. Sacco, Jr., A. G. Dixon, and R. W. Thompson, *Zeolites*, **1993,** *13,* 645–653.
14. H. Lechert, H. in: *Structure and Reactivity of Modified Zeolites* (Ed. P.A. Jacobs), Elsevier, Amsterdam, **1984,** p. 107.
15. J. Warzywoda, and R. W. Thompson, *Zeolites*, **1991,** *11,* 577–582.
16. R. Aiello, F. Crea, A. Nastro, B. Subotić and F. Testa, *Zeolites*, **1991,** *11,* 767–775.
17. B. Subotić, T. Antonić, I. Šmit, R. Aiello, F. Crea, A. Nastro, and F. Testa, in: M.L. Occelli and H. Kessler (Eds), *Synthesis of Porous Materials: Zeolites, Clays, and Nanostructures*, Marcel Dekker Inc., New YorkBaselHong Kong, **1996,** 35–43.
18. E.M. Flanigen, in W.M. Meier and J.B. Uytterhoeven (Eds.), *Molecular Sieves*, *Advances in Chemistry Series No. 121*, American Chemical Society, Washington, D.C., **1973,** 15–23.

19. A. Erdem and L.B. Sand, *J. Catal.* **1979,** *60,* 241.
20. A. Nastro, Z. Gabelica, P. Bodart and J. B. Nagy in S. Kaliaguine and A. Mahay (Eds.), *Catalysis on the Energy Scene*, *Studies in Surface Science and Catalalysis No. 19*, Elsevier, Amsterdam, **1984,** p. 131.
21. A. Nastro, C. Colella and R. Aiello, in B. Držaj, S. Hočevar and S. Pejovnik (Eds.), *Zeolites: Synthesis, Structure, Technology and Application*, *Studies in Surface Science and Catalysis No. 24*, Elsevier, Amsterdam, **1985,** p. 39.
22. G. Giordano, J. B. Nagy, E. G. Derouane, N. Dewaele and Z. Gabelica, in: M. L. Occelli and H. E. Robson (Eds.), *Zeolite Synthesis*, *American Chemical Society Symposium Series No. 398*, American Chemical Society, Washington, D.C., **1989,** p. 587.
23. N. Dewaele, P. Bodart, Z. Gabelica and J. B. Nagy, in B. Držaj, S. Hočevar and S. Pejovnik (Eds.), *Zeolites: Synthesis, Structure, Technology and Application*, *Studies in Surface Science and Catalysis No. 24*, Elsevier, Amsterdam, **1985,** p. 119.
24. A. V. McCormik, A. T. Bell and C. J. Radke, *J. Phys. Chem.*, **1989,** *93,* 1733.
25. A. V. McCormik, A. T. Bell and C. J. Radke, *J. Phys. Chem.*, **1989,** *93,* 1737.
26. V. G. Il'in, N. V. Turutina and V. N. Solomakha, in: P. A. Jacobs and R. A. Van Santen (Eds.), *Zeolites: Facts, Figures, Future, Studies in Surface Science and Catalysis No. 49A*, Elsevier, Amsterdam, **1989,** p. 345.
27. R. M. Barrer, *Zeolites*, **1981,** *1,* 130.
28. J.-L. Guth, and P. Caullet, *J. Chim. Phys.* **1986,** *83,* 155.
29. R. Mostowicz and J. M. Berak in Eds. B. Držaj, S. Hočevar, S. Pejovnik (Eds.), *Zeolites: Synthesis, Structure, Technology and Application, Studies in Surface Science and Catalysis No. 24*, Elsevier, Amsterdam, **1985,** p. 65.
30. Z. Gabelica, N. Blom and E.G. Derouane, *Appl. Catal.*, **1983,** *5,* 227.
31. R. Aiello, F. Crea, A. Nastro and C. Pellegrino, *Zeolites*, **1987,** *7,* 594.
32. A. Erdem and L. B. Sand, in L. V. C. Rees (Ed.), *Proceedings of the Fifth International Zeolite Conference,* Heyden, London, Philadelphia, Rheine, **1980,** p. 64.
33. A. Nastro, R. Aiello and C. Colella, *Ann. Chim.*, **1984,** ***74,*** 579–587.
34. R. Szostak, *Molecular Sieves: Principles of Synthesis and Identification*, Van Nostrand Reinhold, New York, **1989,** p. 51.
35. J. B. Nagy, P. Bodart, I. Hannus and I. Kiricsi, *Synthesis, Characterization and Use of Zeolite Microporous Materials*, Deca Gen Ltd., Szeged, **1998,** p. 59.
36. B. Subotić and A. Graovac, in B. Držaj, S. Hočevar and S. Pejovnik (Eds.), *Zeolites: Synthesis, Structure, Technology and Application*, *Studies in Surface Science and Catalysis*, Elsevier, Amsterdam, **1985,** *24,* 199–206.
37. E. Narita, K. Sato, N. Yatabe and T. Okabe, *Eng. Chem. Prod. Res. Dev*., **1985,** *24,* 507.
38. J. Bronić, B. Subotić, I. Šmit, and Lj. A. Despotović, in P. J. Grobet, E. F. Vansant and G. Schulz-Ekloff (Eds), *Innovation in Zeolite Material Science*, *Studies in Surface Science and Catalysis,* **1988,** *37,* 107–114.
39. B. Subotić, in: M. L. Occelli and H. E. Robson (Eds.), *Zeolite Synthesis*, *American Chemical Society Symposium Series No. 398*, American Chemical Society, Washington, D.C., **1989,** 110–118.
40. B. Subotić, A. Tonejc, D. Bagović, A. Čižmek and T. Antonić in J. Weitkamp, H.G. Karge, H. Pfeifer, W. Hoeldrich (Eds), *Zeolites and Related Microporous Materials: State of Art 1994*, *Studies in Surface Science and Catalysis No. 94A*, Elsevier, **1994,** *94A,* 259–266.
41. T. Antonić-Jelić, S. Bosnar, J. Bronić, B. Subotić, M. Škreblin, *Microporous Mesoporous Mater.*, **2003,** *64,* 21–32.
42. T. W. Swaddle, *Coordination Chemistry Reviews*, **2001,** *219–221,* 665–676.
43. A. T. Bell, in M. L. Occelli and H. E. Robson (Eds), *American Chemical Society Symposium Series No. 398*, American Chemical Society, Washington, D.C., **1989,** *398,* 66–74.
44. P. C. Borthakur and B. D. Chattaray, *J. Therm. Anal.*, **1979,** *17,* 67–70.
45. A. J. Chandwadakar and S. B. Kulkarni, *J. Therm. Anal.*, **1980,** *19,* 313–316.
46. P. K. Dutta and B. Del Barco, *J. Phys. Chem.* **1986,** *108,* 1861.
47. B. L. Yu, A. Dyer and H. Enamy, *Thermochim Acta*, **1992,** *200,* 299.
48. P. K. Dutta, M. Puri and C. Bowers, in M. L. Occelli and H. E. Robson (Eds), *American Chemical Society Symposium Series No. 398*, American Chemical Society, Washington, D.C., **1989,** *398,* 98–104.
49. A. Katović, B. Subotić, I. Šmit, LJ. A. Despotović and M. Ćurić, in M. L. Occelli and H. E. Robson (Eds), *American Chemical Society Symposium Series No. 398*, American Chemical Society, Washington, D.C., **1989,** *398,* 124–129.
50. C. D. Cheng and A. T. Bell, *Catal. Lett.* **1991,** *8,* 305–309.
51. R. I. Walton, R. I. Smith and D. O'Hare, *Microporous Mesoporous Mat.* **2001,** *48,* 79–88.
52. P. A. Jacobs, E. G. Derouane and J. Weitkamp, J. Chem Soc. Chem. Commun. **1981,** 591.
53. E. M. Flanigen, H. Khatami and H. A. Szymanski, *Adv. Chem. Ser.* **1971,** *101,* 201–208.
54. Y. Tsuruta, T. Satoh, T. Yoshida, O. Okamura and S. Ueda, in: A. Iijima and J. W. Ward (Eds.), *New Development in Zeolite Science*, Kodansha Ltd., Tokyo, **1986,** p. 1001.
55. G. Engelhardt, B. Fahlke, M. Mgi and E. Lippmaa, *Zeolites*, **1983,** *3,* 292–300.
56. E. Lippmaa, M. Mgi, A. Samson, G. Engelhardt and A.-R. Grimmer, *J. Am. Chem. Soc.* **1981,** *102,* 4889–95.
57. G. Engelhardt, B. Fahlke, M. Mgi and E. Lippmaa, *Zeolites*, **1985,** *5,* 49–52.
58. W. Wieker and B. Fahlke, in: B. Držaj, S. Hočevar and S. Pejovnik (Eds.), *Zeolites: Synthesis, Structure, Technology and Application*, *Studies in Surface Science and Catalysis No. 24*, Elsevier, Amsterdam, **1985,** *24,* 161–181.

59. A. Katović, B. Subotić, I. Šmit and Lj. A. Despotović, *Zeolites*, **1990,** *10,* 634–641.
60. H. Lechert, P. Staelin and C. Kuntz, *Zeolites*, **1996,** *16,* 149–156.
61. R. J. Moolenaar, J. C. Evans and L. D. McKeever, *J. Phys. Chem.* **1970,** *74,* 3629–34.
62. A. V. McCormik, A. T. Bell and C. J. Radke, *J. Phys. Chem.*, **1989,** *93,* 1741–45.
63. B. Fahlke, D. Mller, and W. Wieker, *Z. Anorg. Allg. Chem.* **1988,** *562,* 141–45.
64. R. F. Mortlock, A. T. Bell and C. J. Radke, *J. Phys. Chem.* **1989,** *95,* 7847.
65. L. A. Bursill and J. M. Thomas, in: R. Sersale, C. Collela and R. Aiello (Eds.), *Recent Progress Report and Discussions: 5th International Zeolite Conference*, Naples, Italy, 1980, Giannini, Naples, **1981,** pp. 25–30

Povzetek

Me-aluminosilikatne hidrogele z molarno sestavo $xMe_2O \times Al_2O_3 \times ySiO_2 \times zH_2O$ (Me = Li, Na, K, Rb and Cs); x = 4.24 – 4.66, y = 2.49 in z = 334.53 – 344.48 (serija a), in x = 9.52 – 10.30, y = 7.91 – 7.95 z = 1073.38 – 1097.29 (serija b) smo pripravili z mešanjem raztopin Me-silikata in Me-aluminata pri sobni temperaturi. Vzorce smo kondicionirali 48 ur pri 25 °C ter nato ločili trdno in tekočo fazo ter obema določili kemijsko sestavo (vsebnosti Me_2O, Al_2O_3 in SiO_2) z AAS. Trdne faze smo dodatno preiskali z XRD, FTIR in DTG. Specifične ravnotežne porazdelitve Me_2O, Al_2O_3 in SiO_2 med trdnimi in tekočimi fazami smo opisali glede na a) vpliv Me ionov na porazdelitev različnih silikatnih anionov in njihovo stopnjo hidroksilacije v izhodnih Me-silikatnih raztopinah ter b) vpliv stopnje hidroksilacije silikatnih anionov v izhodnih Me-silikatnih raztopinah na polikondenzacijske reakcije monomernimi $[Al(OH)_4]^-$ anioni med nastankom gela. Prisotnost ali odsotnost kvazi-kristaliničnih zeolitom-podobnih struktur v matriki gela smo pripisali specifični naravi Li^+ and Na^+ kationov, ki nastanek strukture omogočajo ter K^+, Rb^+ in Cs^+ kationom, ki nastanek strukture preprečujejo.